

Spiral Instabilities in N -body Simulations: Emergence from noise II

J. A. Sellwood,^{1*}

¹*Steward Observatory, University of Arizona, 933 N Cherry Ave, Tucson AZ 85722, USA*

6 January 2020

ABSTRACT

An earlier paper presented the potentially significant discovery that disturbances in simplified simulations of a stellar disc model that was predicted to be stable in linear theory grew to large amplitude over a long period of time. The ultimate appearance of true instabilities was attributed to non-linear scattering by a succession of collective waves excited by shot noise from the finite number of particles. The paper concluded that no finite number of particles, however large, could mimic a smooth disc. As this surprising finding has been challenged as an artifact of the numerical scheme employed, we here present a new calculation of the same model using a different grid geometry that confirms the original behaviour.

Key words: galaxies: evolution — galaxies: structure — galaxies: kinematics and dynamics — methods: numerical

1 INTRODUCTION

Toomre (1981, following Zang 1976) made the remarkable prediction that the half-mass Mestel disc, whose properties are described below (§2), is globally stable to gravitationally-driven disturbances in the stellar distribution. His prediction was based on the usual linear stability analysis of small-amplitude perturbations in which second-order terms are neglected (*e.g.* Kalnajs 1971; Binney & Tremaine 2008). Toomre’s prediction is important since it remains the most interesting, smooth disc model to be predicted to stable.¹ Furthermore, a stable disk model enables phenomena such as swing-amplification to be studied in a global context (Toomre 1981), and can be modified to excite instabilities in a controlled manner (Sellwood & Kahn 1991; Sellwood & Binney 2002; Sellwood & Carlberg 2019).

Sellwood (2012, hereafter S12) presented simulations to test Toomre’s prediction that the unmodified Mestel disc should be stable. The initial behaviour of his larger N simulations (up to $N = 5 \times 10^8$) broadly confirmed Toomre’s prediction, but S12 also reported that all his N -body realizations of this model were ultimately non-linearly unstable. The interesting new phenomenon that eventually dominated his long-duration simulations was caused by the response of the disc to shot noise from the finite number of parti-

cles. He showed (see also Figure 1b of Sellwood & Carlberg 2019) that multiple episodes of swing-amplified shot noise each launched inwardly travelling disturbances that were absorbed at their inner Lindblad resonances. The non-linear scattering of particles as they absorbed energy from each wave, a consequence that is neglected in all linear stability analyses, created a “scratch” (or “scar” *cf.* Sridhar 2019) in the distribution function that enhanced the responsiveness of the disc to subsequent noise-driven disturbances. The extra responsiveness caused the amplitude of successive disturbances to increase slowly at first, but eventually led to a full-blown linear instability.

Fouvry & Pichon (2015) and Fouvry *et al.* (2015) showed that the mildly non-linear behaviour reported by S12 was quantitatively consistent with the predictions of diffusion coefficients computed from the self-gravitating responses to shot noise. Furthermore, linear stability analysis by De Rijcke *et al.* (2019) of the modified $N = 50M$ particle distribution confirmed the same unstable mode that S12 had fitted to data from his simulations.

Because one should always be suspicious of surprising behaviour in simulations, S12 conducted a painstaking search for a possible numerical cause of the new instabilities. But since all his tests employed the same grid geometry, it remains possible that some kind of artifact of the polar grid could be responsible for misbehaviour. Two examples of possible inadequacies are (1) that the sizes of the grid cells on a polar grid increase linearly with radius, causing grid resolution to degrade with increasing radius, and (2) grid aliasing could cause a tightly wrapped trailing wave to seed a tightly wrapped leading disturbance; were this to happen, it would

* E-mail: sellwood@as.arizona.edu

¹ Two stable “composite” disc models were also presented by Kalnajs (1972), but uniformly rotating discs are implausible models of galaxies and are more easily stabilized because they do not support swing amplification.

be a numerical cause of indefinite growth. S12 was aware of these possibilities, which prompted him to test the consequences of halving the grid cell sizes repeatedly, only to find that neither the rate of growth of non-axisymmetric disturbances nor the overall qualitative behaviour depended on grid resolution, as might be expected if either of these hypothesized causes were responsible for misbehaviour. However, a more convincing test would be to check whether the evolution is affected in any way by the choice of grid geometry, which is the purpose of the present paper. Here we show that new a simulation of the same physical model that employed a Cartesian grid behaves in a strikingly similar manner to the corresponding case reported in S12, confirming that the original, somewhat surprising, findings of that paper were not a numerical artifact of the polar grid.

2 TECHNIQUE

2.1 Disc model

The razor-thin Mestel disc used in the studies by Zang (1976) and Toomre (1981) is characterized by a constant circular speed V_0 at all radii. The axisymmetric surface density $\Sigma_0(R) = V_0^2/(2\pi GR)$ would self-consistently yield the appropriate central attraction for centrifugal balance. The lopsided instability of the full mass disc found by Zang (1976) is suppressed when the surface density is halved, with the removed mass added to a rigid halo to maintain centrifugal balance. These authors employed the distribution function (DF) given by Toomre (1977) and Binney & Tremaine (2008), which for the half-mass disk is

$$f(E, L_z) = 0.5 \begin{cases} F(L_z/R_0 V_0)^q e^{-E/\sigma_R^2} & L_z > 0 \\ 0 & \text{otherwise,} \end{cases} \quad (1)$$

where R_0 is a reference radius, $q = V_0^2/\sigma_R^2 - 1$, and the normalization constant is

$$F = \frac{1}{GR_0} \frac{(q/2 + 0.5)^{q/2+1}}{\pi^{3/2}(q/2 - 0.5)!}. \quad (2)$$

Choosing $q = 11.44$ yields a Gaussian distribution of velocities such that the half-mass disc has $Q = 1.5$. Toomre further multiplied the DF f by the double taper function

$$T(L_z) = \left[1 + \left(\frac{R_0 V_0}{L_z}\right)^\nu\right]^{-1} \left[1 + \left(\frac{L_z}{R_1 V_0}\right)^\mu\right]^{-1}, \quad (3)$$

to create a central cut out and an outer taper having mean radii R_0 and R_1 respectively, while maintaining the centripetal acceleration $-V_0^2/R$ everywhere. Setting the taper indices $\nu = 4$ and $\mu = 5$ yielded an idealized, smooth disc model that Toomre claimed possessed no small amplitude unstable modes. S12 chose $R_1 = 11.5R_0$, and limited the radial extent of the disc by an energy cut-off that eliminated particles having sufficient energy to pass $R = 20R_0$. As usual, we adopt units such that $G = V_0 = R_0 = 1$.

2.2 Numerical method

Since the behaviour in simulations with unrestricted forces can be quite complicated, S12 simplified his experiments by including only force terms that arose from bisymmetric disturbances in the particle distribution. As all stability

Table 1. Numerical parameters

Cartesian grid size	1024 × 1024
R_0	25 grid units
Softening length	$R_0/8$
Number of particles	5×10^7
Basic time-step	$0.025(R_0/V_0)$
Time step zones	5

analyses take advantage of the separation of individual sectoral harmonics in the determination of the gravitational field (Binney & Tremaine 2008), Sellwood's simplification mirrored that of the prediction he was attempting to verify. The ease with which restrictions to the range of sectoral harmonics that contribute to the gravitational field can be accomplished on the polar grid made it a natural choice for the calculations presented in S12.

S12 therefore employed a 2D polar grid having N_R rings and N_A spokes. The grid rings were spaced as

$$R_g(u) = h_R (e^{\alpha u} - 1), \quad (4)$$

with $\alpha = 2\pi/N_A$, u taking integer values in the range $0 \leq u \leq N_R - 1$ so that $R_g(0) = 0$, and the quantity h_R defines the spatial scale. Thus the fixed angular separation of the spokes, together with the almost linear increase in the radial spacing of the grid rings, causes grid cells with $e^{\alpha u} \gg 1$ to have similar shapes but to increase in size with radius. S12 chose $h_R = R_0/8$ and $(N_R, N_A) = (106, 128)$ for most simulations.

In order to test for possible misbehaviour that might have been caused by that choice of grid, we here report fresh calculations of the same physical model using a 2D Cartesian grid. The FFT method to determine the gravitational acceleration, with grid doubling in both x and y , and the standard cloud-in-cell (*i.e.* linear) interpolation scheme is described in Sellwood (2014). The numerical parameters of the two simulations presented here are given in Table 1. For efficiency, the code employs block time steps, with the time-step being doubled in each of a series of annular zones whose boundaries lie at radii that are themselves successively increased by factors of two, as appropriate for a flat rotation curve.

In order to check the results of S12, we must again restrict the accelerations to those arising only from bisymmetric disturbances in the mass distribution. We adopted the following two stratagems to accomplish this goal on the Cartesian grid.

First, we began by computing an exactly smooth mass distribution on the grid, created by integrating the tapered DF (eqs. 1 & 3) over all velocities. The mass assigned to each grid point is therefore free from all shot noise that would arise from any finite number of particles. A simulation with a finite number of particles then proceeds by assigning their masses to the grid in the usual manner at every step, after which we subtract the pre-calculated smooth mass distribution. Consequently, the gravitational field determined from this residual mass distribution is that arising only from particle shot noise and its associated collective response. To ensure dynamical equilibrium, we added the analytic central attraction of the Mestel disc model, $a_R = -V_0^2/R$, to these grid-determined acceleration components for each particle at each step, as was also done in S12.

Second, there is no simple way to restrict the distur-

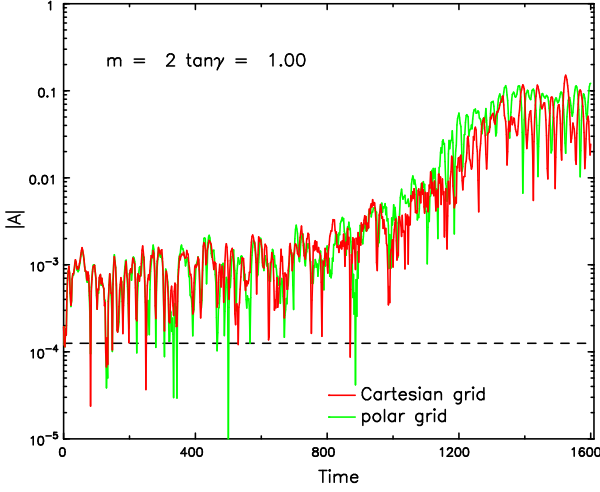


Figure 1. The amplitude evolution of the given logarithmic spiral coefficient (eq. 6) in run 50C on the Cartesian grid (red curve) compared with the same quantity from run 50 reported in S12 (green curve). The dashed line indicates the expectation value $\langle |A| \rangle = (\pi/4N)^{1/2}$ if the particle distribution were random.

bance forces to be perfectly bi-symmetric, but an excellent approximation to this goal is easy to accomplish. Taking advantage of the 4-fold rotation symmetry of the grid, we replaced the mass assigned to each grid point $d(i, j)$ by the following average at every step

$$d_4(i, j) = \frac{1}{4} [d(i, j) - d(-j, i) + d(-i, -j) - d(j, -i)], \quad (5)$$

with the indices (i, j) reckoned from the grid centre. A simple average $d_2(i, j) = \frac{1}{2} [d(i, j) + d(-i, -j)]$, would retain contributions from all even sectoral harmonics with $m \geq 2$, and we have found that disturbances grow somewhat more rapidly when the $m = 4$ term in particular contributed to the disturbance forces. However, eq. (5) also suppresses all $m = 4j$ terms, with integer $j \geq 1$. The first surviving term is bisymmetric, and although all $m = 2 + 4j$ terms also contribute to the disturbance forces, the half-mass Mestel disk can support only very mild responses to disturbances having rotational symmetries $m \geq 6$, since Toomre's swing-amplification parameter $X = 4/m$ in the half-mass Mestel disc.

3 RESULTS

Starting from the same file of 50M initial particle coordinates that was used for model 50 in S12, we have used a Cartesian grid, with the modifications just described, to recompute the evolution to $t = 1600$. We denote this calculation as run 50C. Note that both runs 50 and 50C were long integrations; the orbit period at $R = 10$, half-way out in the disk, is 20π in these units.

Unlike with the polar grid, it is not straightforward to report the amplitude of non-axisymmetric disturbances as function of radius in simulations run on the Cartesian grid. Thus we here employ a different measure from that presented in S12: the amplitude of a global logarithmic transform of the particle positions. For equal mass particles, the

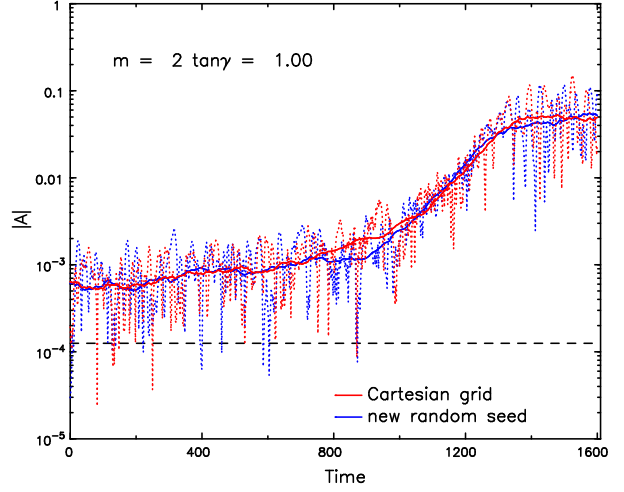


Figure 2. The dotted curves are for run 50C (red), reproduced from Figure 1, and run 50R (blue) that started from a different random draw from the DF. The solid curves are simple running averages. Both simulations were run on the Cartesian grid with the parameters listed in Table 1 and with disturbance forces restricted to $m = 2 + 4j$ as described in the text.

complex coefficients are evaluated as

$$A(m, \gamma, t) = \frac{1}{N} \sum_j e^{im(\phi_j + \tan \gamma \ln R_j)}, \quad (6)$$

where (R_j, ϕ_j) are the polar coordinates of the j -th particle at time t , and γ is the angle between the tangent to an m -arm logarithmic spiral and the radius vector, with positive values for trailing spirals.

Figure 1 compares the evolution of $|A(2, \pi/4, t)|$ from run 50C (red curve) with the same quantity from the original run 50 (green curve) reported in S12, which employed the polar grid. In both cases, the dominant disturbance forces were restricted to $m = 2$. The initial amplitude is consistent with random, as marked by the dashed line, but rises by a factor of several in the first few dynamical times as the gravitational forces polarize the particle distribution (Toomre & Kalnajs 1991). Although this Figure is for $\tan \gamma = 1$, implying a trailing pitch angle of 45° , the agreement between the two simulations is similarly impressive for $-1 \leq \tan \gamma \leq 3$.

In order to show the good agreement of even the high temporal frequency amplitude variations, we have not attempted to smooth these curves. The rapid changes arise from the superposition of several disturbances, each having different pattern speeds, which causes alternating reinforcement and cancellation in the global transform (6). Since the two simulations began with the same file of particle coordinates, they have the exact same initial noise spectrum. The two curves track each other perfectly in the early stages, indicating identical dynamical responses to the noise. Since the system being simulated is stochastic (Sellwood & Debattista 2009), minor differences emerge at later times that probably arise from the cumulative effects of round-off error that must differ on the two grids, but the overall evolution remains decisively similar.

Because all simulations employ approximations both to compute the gravitational field and to integrate the motion

of the particles, none can be completely free from numerical artifacts. But flaws arising from the approximations associated with the calculation of the field and interpolation between grid points, which differ significantly between the two grid geometries, are most unlikely to drive such similar evolution.

It is evident from Figure 1 that the qualitative evolution is unaffected by stochasticity, but in order to show that there is nothing odd about the file of particles used for both models, we present a second case, model 50R, that started from a different random draw from the DF. (S12 reported that he had made a similar test using the polar grid, but did not present the result.) The amplitude of the logarithmic spiral in run 50C (red line) is compared with that from run 50R (blue line) in Figure 2, and in this Figure we have also smoothed the data in order to emphasize the agreement on longer time scales.

The overall behaviour of the disturbances in the three simulations 50, 50C and 50R is remarkably similar. Aside from the high frequency variations, all three runs manifest a gradually increasing amplitude to $t \simeq 800$ followed by a more rapid increase, which peaks at $t \simeq 1300$, by which time the inner disk is developing a bar in all cases. The close agreement at all times implies that the processes of swing-amplification, resonance scattering, and enhanced responsiveness identified by S12 occur to almost exactly the same extent, and with the same time dependence, in all three of these calculations. Together with the dependence on particle number and the other tests reported in S12, these new simulations strongly support the earlier contention that the gradual emergence of instabilities is physically real and does not result from inadequacies in the numerical schemes.

4 CONCLUSIONS

The spectacular agreement, illustrated in Figure 1, between the result presented here and one of those reported by Sellwood (2012), confirms that the secular rise in the amplitude of disturbances does not result from artifacts of the grid used to compute gravitational accelerations. The earlier reported tests involving variation of the time step, the number of time step zones, locations of the zone boundaries, grid resolution, and random seed (and also Figure 2) were all similarly reassuring. These numerical checks leave little room to doubt the validity of the results presented in S12. The subsequent analyses by Fouvry & Pichon (2015), Fouvry *et al.* (2015), De Rijcke *et al.* (2019) and Sridhar (2019) have also provided welcome backup to the findings of S12.

Note that Toomre & Kalnajs (1991) reported only “an enhanced responsiveness” and not a final runaway to instability in their long duration simulations that employed the sheared sheet (local) approximation with periodic boundary conditions. However, in order to maintain long-term responsiveness, those authors added a mild radial damping term to the forces acting on the particles. That seemingly innocent addition almost certainly damped away the consequences of resonant scattering, thereby preventing their simulations from manifesting any true instabilities. D’Onghia *et al.* (2013) employed 10^8 particles in a global simulation of an unperturbed low mass disc, concluding it was “stable” because no visible features appeared after “two to three galac-

tic years.” But their test was of too short duration for the behaviour reported in S12 to have reached large amplitude.

The physical implication of the finding in S12, and confirmed here, is that any differentially rotating disc of particles will eventually be destabilized as a result of non-linear scattering by collective waves seeded by shot noise, no matter how many particles are employed.

ACKNOWLEDGEMENTS

The author acknowledges a vigorous correspondence with Agris Kalnajs, which was the principal motivation for this work. He is also grateful to an anonymous referee for helpful comments, to Ray Carlberg for advice, and to Steward Observatory for their continued hospitality.

REFERENCES

- Binney J. & Tremaine S. 2008, *Galactic Dynamics* 2nd ed. (Princeton University Press, Princeton NJ) (BT08)
- De Rijcke, S., Fouvry, J.-B. & Pichon, C. 2019, MNRAS, **484**, 3198
- D’Onghia, E., Vogelsberger, M. & Hernquist, L. 2013, ApJ, **766**, 34
- Fouvry, J.-B., Binney, J. & Pichon, C. 2015, ApJ, **806**, 117
- Fouvry, J.-B. & Pichon, C. 2015, MNRAS, **449**, 1928
- Kalnajs, A. J. 1971, ApJ, **166**, 275
- Kalnajs, A. J. 1972, ApJ, **175**, 63
- Sellwood, J. A. 2012, ApJ, **751**, 44 (S12)
- Sellwood, J. A. 2014, arXiv:1406.6606 (on-line manual: <http://www.physics.rutgers.edu/~sellwood/manual.pdf>)
- Sellwood, J. A. & Binney, J. J. 2002, MNRAS, **336**, 785
- Sellwood, J. A. & Carlberg, R. G. 2019, MNRAS, **489**, 116
- Sellwood, J. A. & Debattista, V. P. 2009, MNRAS, **398**, 1279
- Sellwood, J. A. & Kahn, F. D. 1991, MNRAS, **250**, 278
- Sridhar, S. 2019, ApJ, **884**, 3
- Toomre, A. 1977, ARA&A, **15**, 437
- Toomre, A. 1981, In “The Structure and Evolution of Normal Galaxies”, eds. S. M. Fall & D. Lynden-Bell (Cambridge, Cambridge Univ. Press) p. 111
- Toomre, A. & Kalnajs, A. J. 1991, in *Dynamics of Disc Galaxies*, ed. B. Sundelius (Gothenburg: Göteborgs University) p. 341
- Zang, T. A. 1976, PhD thesis., MIT

This paper has been typeset from a $\text{\TeX}/\text{\LaTeX}$ file prepared by the author.